EFSAT
An Exact and Efficient Triangle Intersection Test Hardware

Andreas Raabe, Jan Tietjen, Joachim K. Anlauf
Technical Computer Science, University of Bonn, Römerstr. 164, 53117 Bonn, Germany
{*raabe,tietjen,anlauf*}*@cs.uni-bonn.de*

Keywords: Intersection Test, Hardware Acceleration, Fixed-Point, Exact

Abstract: Software implementations that test two triangles for intersection often favour speed over exact calculation. They leave it to the user to choose an exact or a fast test depending on the domain of application. Hardware implementations can not opt to make this distinction since users will always expect an accelerator hardware to be applicable in all possible settings. This paper introduces a novel approach towards exact intersection testing of triangles. It is based on the separating axes test and lends itself well to hardware implementation. To be integrable into a hierarchical collision detection design this test needs to be extremely resource efficient. Thus, it does not iterate until an exact solution is found, but instead categorises results as correct and possibly incorrect. It is implemented using 18-bit fixed-point numbers, while still maintaining resolutions that can keep up with double-precision floating-point implementations. The proposed test is integrated into a hierarchical collision detection FPGA-design accelerating collision queries by an order of magnitude. In a realistic benchmark less than 0.9% of possibly incorrect results are reported without impairing system performance.

1 INTRODUCTION

In physically-based simulation most of the processing effort is spent on collision detection (Plante et al., 2001). Hence hardware acceleration of collision queries significantly speeds-up the overall simulation and liberates the CPU for other tasks. Since surfaces are often composed of triangles, a last step in processing the query is usually intersection testing of triangle pairs. When using hierarchical or spacial subdivision approaches only a relatively small number of triangles will be singled out for testing. This and the concurrent processing of the hierarchy renders the overall performance independent of the delay of the triangle intersection test. Still, it is highly beneficial to implement it in hardware as well, since it will reduce the number of triangles transferred back to the host. This reduces the delay caused by bus transfers which has significant impact on overall performance.

Software implemented algorithms for testing two triangles for intersection often favor speed over exact calculation. Examples for this are the well known intersection tests of Held (Held, 1996) and Möller (Möller, 1997). They leave it up to the user to choose an exact or a fast test depending on the domain of application. Hardware implementations can not opt to make this distinction since users will always expect an accelerator hardware to be applicable in all possible settings. Known approaches for exact collision detection, on the other hand, are usually iterative in nature. In general this iterativeness arises through the use of arbitrary precision libraries like CORE (Karamcheti et al., 1999) or LEDA (Mehlhorn and Schirra, 2001) in standard algorithms like the ones stated above. This renders every arithmetic operation a potential iteration over the necessary precision. (Robbins and Whitesides, 2003) uses Shewchuk's orientation test (Shewchuk, 1997) in combination with Möller's intersection test. This is more elegant, since it solely needs to iterate the calculation of the 3D orientation predicate given as the sign of a polynomial of degree 3 in the coordinate values of four points. A well known fact in hardware development is that unrolling iterative algorithms renders them very resource consuming. Since in general one will want to operate the triangle intersection concurrently to a hierarchy or a spatial subdivision traversal, they both need to be small to fit into the same chip. This avoids additional delay caused by inter-chip communication. A very fast and yet hardware efficient hierarchical collision detection architecture based on k-DOPs was proposed by (Raabe et al., 2006). It is also provably exact, thus it does not return any false reports of non-collision. It will be used in the following as a basis and the proposed exact intersection test will be integrated into the overall design. Usage of hierarchical intersection test yields a logarithmic average run-time in realistic scenarios (Weller et al., 2006). An AABB based broad-phase collision test was implemented in hardware in (Woulfe et al., 2007). It could be applied prior to the hierarchy traversal in future implementations.

2 EFSAT

2.1 Separating Axes Test

The separating axes approach as proposed in (Gottschalk, 1996) tests two convex polytopes for intersection by projecting them onto a set of test axes. If the projections do not intersect it follows that the axis is the normal of a plane separating the polytopes. If neither any normal of any of the faces, nor any cross products of edges of both polytopes are a separating axis then the polytopes intersect.

Triangles can be interpreted as degenerated polytopes in 3D and thus the SAT approach can be applied to them. Let $\widetilde{A}$ and $\widetilde{B}$ be two triangles. In general $\widetilde{A}$ and $\widetilde{B}$ will life in different reference frames (RFs). To test them for intersection, we need to transform them into a common RF. Let this common RF be that of $\widetilde{A}$ without loss of generality and let M be the according transformation matrix. Let the resulting triangles be B (with vertices W_0, W_1, and W_2) and $A = \widetilde{A}$ (with vertices V_0, V_1, and V_2).

Using around indexing, the normals n_A, n_B and the cross products $C_{k,l}$ can now be calculated as follows.

$$\begin{aligned} n^A &:= (V^1 - V^0) \times (V^2 - V^0) \\ n^B &:= (W^1 - W^0) \times (W^2 - W^0) \\ C_{k,l} &:= (V^{k+1} - V^k) \times (W^{l+1} - W^l) \end{aligned} \quad (1)$$

Then the triangles' points are projected onto any test axis L out of this set by

$$p_{V^k} := V^k * L \quad p_{W^l} := W^l * L \quad (2)$$

The projection intervals on the axis are

$$\begin{aligned} I_A &:= [\min\{p_{V^0}, p_{V^1}, p_{V^2}\}, \max\{p_{V^0}, p_{V^1}, p_{V^2}\}] \\ I_B &:= [\min\{p_{W^0}, p_{W^1}, p_{W^2}\}, \max\{p_{W^0}, p_{W^1}, p_{W^2}\}] \end{aligned} \quad (3)$$

If I_A and I_B do not intersect a separating axis is found. It follows that the triangles are non-intersecting. If none of the axes is separating the triangles do intersect.

This test lends itself well to resource efficient hardware implementation as was discussed in (Raabe et al., 2008). The structure of this non-exact test serves as a basis for the exact intersection test EFSAT proposed in the following.

2.2 Pre-Processing

This calculation will (of course) not be computationally exact if it is implemented using fixed-point or floating-point types. Thus the images resulting from the projections will differ from the mathematically correct image. Size and sign of the error depend on the size of the numbers and the rounding mode used for arithmetic operations (e.g., IEEE floating-point arithmetic defaults to rounding 0.0001 to 0.00 (error$= 0.0001$), and 0.001 to 0.01 (error$= -0.001$)).

To enable use of fixed-point data types it is imperative to normalize the objects to prevent a tremendous loss of precision. Thus, all triangles are normalized relatively to the size of the biggest one. To enable bounding of all subsequent calculations assume that a hierarchical bounding-volume test was executed prior to the triangle intersection test. We are using k-DOPs as bounding-volumes, and thus obtain $2\sqrt{3}$ as a bound on the maximum distance of triangles fed into the intersection test. Thus, numbers with 4-bit integral digits are used. Any other bound will work as well.

2.3 Fixed Point Interval Arithmetic

An obvious solution is using an arbitrary precision datatype. As previously discussed this is very resource consuming when implemented in hardware. Therefore we choose not to provide an exact solution for every query, but to categorize the results in exact and possibly incorrect. Due to the grave space restriction imposed by the FPGA-implementation we use fixed-point arithmetic, and exploit that we have complete control over the rounding modes and bit width of the numbers.

Let $a^{n,k}$ be a fixed-point number of length n, of which the k most significant bits are the integral part of the number. $m := n - k$ is the number of fractional bits. Let $\oplus$ furthermore denote bit concatenation and let $a \in \mathbb{R}$, $-2^{k-1} \leq a < 2^{k-1} - 1$. Now let $\lfloor a^{n,k} \rfloor$ be the next smaller or equal fixed-point number of the given dimensions and $\lceil a^{n,k} \rceil$ be the next greater one. The fixed-point resolution is then given by

$$EPS^{n,k} := \lceil a^{n,k} \rceil - \lfloor a^{n,k} \rfloor = 0.\underbrace{0 \cdots 0}_{m-1}1 \quad (4)$$

Now we can initialize fixed-point intervals, so that they contain the input data.

$$A^{n,k}(a) := \left[\underline{A^{n,k}}, \overline{A^{n,k}}\right] = \left[\lfloor a^{n,k} \rfloor, \lceil a^{n,k} \rceil\right] \quad (5)$$

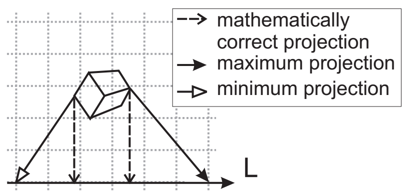

Figure 1: The actual projection using interval arithmetic can be interpreted as a projection of the point intervals onto the original axis. Then the minimum projection is underestimated and the maximum projection is overestimated.

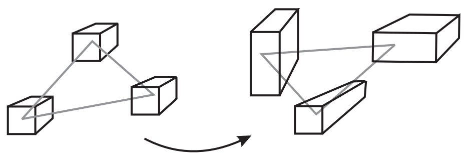

Figure 2: Transforming one triangle into the reference frame of the other using fixed-point numbers contributes to the derivation from the mathematically correct result. This is respected in the size of the coordinate intervals.

If this is done to all coordinates of a triangle point the resulting intervals can be visualized as a cube aligned with the discretization grid induced by the fixed-point data-type.

Now operators $\otimes \in \{+, \cdot, -\}$ can be defined on intervals in a way, that the resulting interval contains all possible outcomes of applying the operation to any pair of numbers out of the intervals. Since linear operators are used exclusively these operations can be implemented very resource efficient using case discrimination based on the signs of the interval bounds. Since this is simple, but a bit lengthy it is left out here. To prevent intermediate results from becoming to large in bit-length they are reduced to the original bit-length by rounding. This is easily done by rounding towards $-\infty$ and, if it is supposed to be an upper limit $EPS^{n,k}$ of the target type is added.

Now the projection Eq. 2 is applied to the interval points using these interval operators and a test axis also described using intervals. This can geometrically be interpreted as a projection onto the original test axis where the projection of the maximum possible value of the point will be overestimated to avoid rounding errors. The minimum value will be underestimated accordingly. Fig. 1 illustrates this.

2.4 Testing Interval Images for Intersection

After applying the previously discussed data types and operators, the points of the triangles can be projected using interval arithmetic. Since again intervals result it is no longer clear, how they need to be transformed into images. Therefore it is necessary to geometrically interpret the presented algorithm.

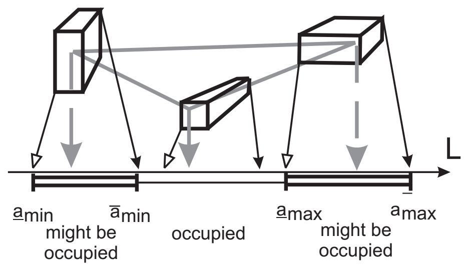

(a)

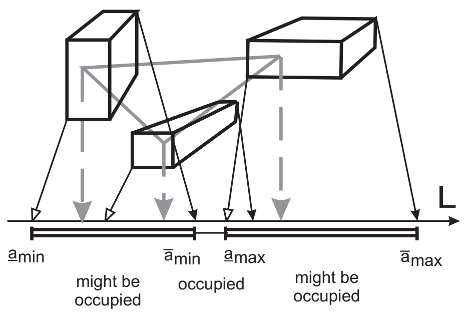

(b)

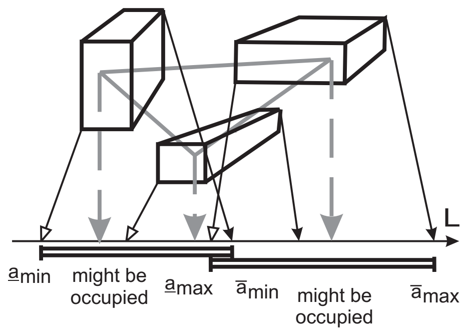

(c)

Figure 3: Projecting the point intervals onto the test axis can lead to different configurations of the resulting images of the interval boundaries. Which case applies depends on the distance of the point intervals and the relative distance to the test axis.

Consider Fig. 2. Initializing the fixed-point intervals with point coordinates will turn the points into cubes of $EPS^{n,k}$ side length. Transforming triangle B into A's reference frame will turn those cubes into cuboids, whose side lengths depend on the absolute values of the original coordinates and of the matrix entries. The actual projection of these cuboids results in a minimum and a maximum projection each. From these we can derive the projection interval Eq. 3. The boundaries of the projection interval are now intervals themselves, denoting the range the extremal points of the triangle could possibly be projected on. The projection intervals can be pairwise intersecting or not.

Fig. 3 illustrates some of the cases that can occur.

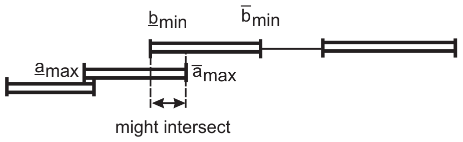

Figure 4: Only if two intervals that contain the minimum *and* the maximum projection interval of one of the triangles (e.g., A_{min} and A_{max}) each are non-intersecting it can be derived, that the triangles are also non-intersecting.

Which case applies depends on the distance of the coordinate intervals and the relative distance to the test axis. The closer the point intervals are located and the farther a point is from the test axis the more probable it is that the projections of the point intervals intersect.

If the images of the point intervals are separated, it can be derived which point contributes to the maximum and the minimum interval (Fig. 3(a)). If neighboring images intersect this is no longer possible (Fig. 3(b)). Still, in both of these cases a line segment which is definitively occupied by the image can easily be identified. This will be used to identify definitive intersections with another triangle image. Fig. 3(c) shows a configuration were all three images of the point intervals intersect. No line segment is occupied by the image for sure.

But in any case the greatest point projection can vary only between the greatest maximum projection and the greatest minimal projection. Let these be denoted by $\overline{a}_{max}$ and $\underline{a}_{max}$. The smallest point projection is located between the smallest minimum projection and the smallest maximum projection. Let these be denoted $\overline{a}_{min}$ and $\underline{a}_{min}$ respectively. Let the minimum (and maximum) interval of a triangle A be denoted by $A_{min} := [\underline{a}_{min}, \overline{a}_{min}]$ (and $A_{max} := [\underline{a}_{max}, \overline{a}_{max}]$)

Thus the images of the triangles become 'blurred'. They now become intervals of intervals (compare Eq. 3). Thus, it is now longer obvious, which configurations of two triangle projections need to be interpreted as intersecting and which implicate that the triangles are non-intersecting.

The latter is the simpler of the two cases and thus is tackled first. Consider the two intervals that contain the extreme boundaries of each projected triangle $A = [\underline{a}_{min}, \overline{a}_{max}]$ and $B = [\underline{b}_{min}, \overline{b}_{max}]$). Only if these two intervals are non-intersecting it can be derived, that the triangles are also non-intersecting, since in all remaining cases the mathematically correct projections might intersect (see Fig. 4). This accounts to the following criterion:

$$(\underline{b}_{min} > \overline{a}_{max}) \vee (\underline{a}_{min} > \overline{b}_{max}) \Rightarrow \text{separation} \qquad (6)$$

Checking for intersections is more complicated. Especially configurations were triangle images do not occupy a line segment for sure (see Fig. 3(c)) are causing problems. If this applies to both triangles it is impossible to identify cases were the images intersect for sure. To cover all remaining configurations multiple cases have to be discriminated. Consider Fig. 5. If $x \in A_{max}, y \in B_{max}$ implies that $x < y$, then the projections will only intersect for sure, if $x \in A_{max}, y \in B_{min} \Rightarrow y < x$. This accounts to the following criterion:

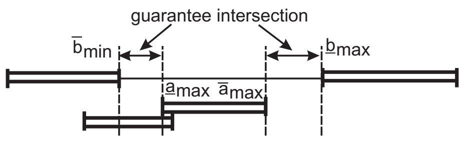

Figure 5: If $x \in A_{max}, y \in B_{max}$ implies that $x < y$, then the projections will intersect for sure only if $x \in A_{max}, y \in B_{min} \Rightarrow y < x$.

$$\text{case}\,(\overline{a}_{max} < \underline{b}_{max}) : (\overline{b}_{min} < \underline{a}_{max}) \Leftrightarrow \text{intersection} \qquad (7)$$

Very analogously further criteria can be identified:

$$\begin{aligned} \text{case}\,(\overline{b}_{max} < \underline{a}_{max}) &: (\overline{a}_{min} < \underline{b}_{max}) \Leftrightarrow \text{intersection} \\ \text{case}\,(\overline{a}_{min} < \underline{b}_{min}) &: (\underline{a}_{max} < \overline{b}_{min}) \Leftrightarrow \text{intersection} \\ \text{case}\,(\overline{b}_{min} < \underline{a}_{min}) &: (\underline{b}_{max} < \overline{a}_{min}) \Leftrightarrow \text{intersection} \end{aligned} \qquad (8)$$

If the images are not definitively separate, but none of the above cases applies we know that the maximum intervals A_{max} and B_{max} intersect and that the minimum intervals A_{min} and B_{min} intersect. In this case we have to ensure, that the surely occupied spaces do overlap, before an intersection can be derived.

$$\begin{aligned} &\text{All remaining cases :} \\ &(\overline{a}_{min} < \underline{b}_{max}) \wedge (\overline{b}_{min} < \underline{a}_{max}) \Leftrightarrow \text{intersection} \end{aligned} \qquad (9)$$

If the images are neither intersecting nor separated for sure, the result of the axis test is marked as possibly incorrect. We experimented with various approaches to provide an educated guess on the exact outcome, but none yielded satisfying results. Thus the simplest solution was chosen and all possibly incorrect results are assumed to be intersections. This is the weaker assumption and will be corrected by any definitive separating axis found, since in this case the triangles do not intersect for sure. If no separating axis was found, but any of the axes tests returned a possibly incorrect intersection the overall result of the triangle intersection test is 'possibly incorrect intersection'. This enables the user to decide on how to proceed. Here an exact software intersection test could be applied for example. This way the number of possibly incorrect results has a major impact on the overall performance and must be decreased as much as possible, without impairing resource consumption.

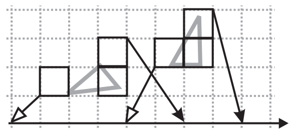

Figure 6: Two triangles that are relatively far from each other considering their sizes. Since they are very small considering the discretization grid induced by the data-type used for the images, the latter still intersect.

2.5 Decreasing the Number of Possibly Wrong Results

The target architecture is a Xilinx Virtex II (XC 2V6000, speed grade -4) on an Alpha Data ADM-XRC-II board with 256 MB DDR-RAM at 100MHz clock frequency. The FPGA features 144 18-bit multipliers and 6 million gate equivalents. Cascading the multipliers to yield bit widths up to 32-bit is prohibitively expensive since it quadruples the number of multipliers used. For benchmarking we integrated the previously introduced design into the hierarchical collision detection architecture presented in (Raabe et al., 2006). We used two identical objects (a car headlight) with 5947 triangles. They are placed in different distances from each other and with different rotations. For each constellation, the time to detect all intersecting triangles is determined. Due to the 18-bit restriction this yields relatively poor results. In this simulation only 16.8% of the queries are exact outcomes. This is unacceptable since it implies that the host PC needs to retest almost all triangle pairs. Therefore a very efficient and effective optimization is proposed in the following. We already normalized the triangles in Sec. 2.2 to enable fixed-point implementation. Still there can be very small triangles compared to the largest one. In the presented framework triangles of sizes close to the fixed-point resolution cause numerical problems, even if the triangles are not closely located with respect to their sizes (Fig. 6). To avoid such configurations the triangle pair can be re-normalize individually on-chip prior to the actual intersection test. This decreases the fixed-point resolution relatively to the distance of the triangles.

One way to accomplish this is to shift the barycenter of the triangles into the origin and stretch them to the outer limits of the fixed-point domain. The latter can be done individually for the coordinate axes to maximize the effect without impairing the outcome of the collision query. To enable efficient implementation, this is approximated by shifting an arbitrary point of the triangles into the origin and shifting the rest consistently. Afterward bit-wise or is applied to the absolute values of the coordinates of all 6 triangle points for their x-,y-, and z-coordinates. The number

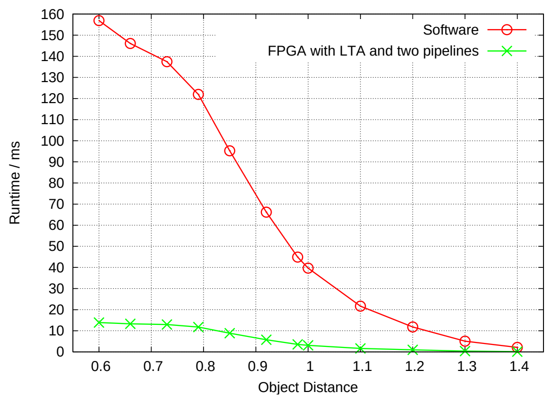

Figure 7: The EFSAT implementation is integrated into a hierarchical collision detection accelerator hardware. The overall design still yields a speed-up of an order of magnitude compared to a state-of-the-art software implementation. The latter does not provide categorization of exact results or any guarantees on correctness.

of leading zeros now denotes the number of bits insignificant for the further calculation. All coordinates are shifted accordingly. Now only the matrix multiplication that transforms $\widetilde{B}$ into A's reference frame is implemented in 32-bit precision. The projection itself is done in 18-bit. Using this scheme 99.1% of the results are exact. This will suffice for the vast majority of applications and enables retesting in all others without impairing the overall performance.

3 Results

3.1 Comparing EFSAT to Möller and SAT

The overall design still yields a speed-up of an order of magnitude compared to a state-of-the-art software implementation (Zachmann, 1998) of a hierarchical collision detection running on a system with an identical memory interface (see Fig. 7). The latter does neither provide categorization of exact results, nor does it provide any guarantees on correctness.

In terms of precision the presented approach can even compete with double precision floating-point implementations of the Möller and the SAT approach. Table 3.1 shows a comparison of the three approaches. As can be seen there exist cases where SAT and Möller disagree. Even in some of these cases the approach presented in this paper provides a definitive answer to the query.

3.2 Resource Consumption

Implemented in VHDL and synthesized, placed and routed with Xilinx ISE 8.1 the design's resource consumption is extraordinarily modest. It uses a total of only 72 18-bit multipliers and 48% of available gates.

EFSAT	Möller	SAT	%
Sep.	Sep.	Sep.	70.93
Sep.	Sep.	Int.	0
Sep.	Int.	Sep.	0.02
Sep.	Int.	Int.	0
Int. (p.i.)	Sep.	Sep.	0.13
Int. (p.i.)	Sep.	Int.	0
Int. (p.i.)	Int.	Sep.	0.04
Int. (p.i.)	Int.	Int.	0.77
Int.	Sep.	Sep.	0
Int.	Sep.	Int.	0
Int.	Int.	Sep.	0
Int.	Int.	Int.	28.13

Table 1: Comparing EFSAT with double precision floating-point implementations of Möller and SAT.

4 CONCLUSION

This paper presents the EFSAT approach, a fixed-point hardware implementation of the SAT algorithm, which categorizes its results into exact and possibly incorrect. An additional optimization improves the resolution of the algorithm, so that it can compete with double precision floating-point implementations of Möller's algorithm and the standard SAT. The approach is extremely resource efficient. It was implemented and tested in VHDL. It utilizes a total of only 72 18-bit multipliers and 48% of available gate equivalents. This enables fitting it into a Xilinx Virtex-II XC 2V6000 together with a hierarchy traversal module. The overall design is ten times faster than a state-of-the-art software implementation running on a system with identical memory bandwidth, which does not provide any guarantees on correctness or categorization of the results. This renders the EFSAT implementation resource efficient, fast, and exact.

5 FUTURE WORK

Due to definition 1 every test axis is orthogonal to at least two triangle edges. Thus the projections of the two triangle points defining this axis are identical. This is exploited in the original SAT-test to reduce the number of projections and comparisons. It remains unclear if this holds for the given algorithm as well and thus will be evaluated.

In all our experiments EFSAT returns correct answers to collision queries concerning colinear triangles, although only 11 axes are tested instead of the 17 necessary for this in the original SAT. It remains an open problem if this can be generalized.

Currently we are working on a software implementation of the SAT algorithm using interval arithmetic and floating-point numbers to provide a fast and precise arithmetic filter.

REFERENCES

Gottschalk, S. (1996). Separating Axis Theorem. Technical Report TR-96-024.

Held, M. (1996). ERIT – A collection of efficient and reliable intersection tests. Technical Report, University at Stony Brook.

Karamcheti, V., Li, C., Pechtchanski, I., and Yap, C. (1999). A core library for robust numeric and geometric computation. In *SCG '99*, New York, USA. ACM.

Mehlhorn, K. and Schirra, S. (2001). Exact computation with leda_real - theory and geometric applications. In *Symbolic Algebraic Methods and Verification Methods*, pages 163–172.

Möller, T. (1997). A Fast Triangle-Triangle Intersection Test. *journal of graphics tools*, 2(2):25–30.

Plante, E., Cani, M.-P., and Poulin, P. (2001). A layered wisp model for simulating interactions inside long hair. In *Computer Animation and Simulation 2001*, Computer Science.

Raabe, A., Hochgürtel, S., Zachmann, G., and Anlauf, J. K. (2006). Space-Efficient FPGA-Accelerated Collision Detection for Virtual Prototyping. In *Design Automation and Test (DATE)*, pages 206–211, Munich, Germany.

Raabe, A., Nett, A., and Niers, A. (2008). A Refinement Case-Study of a Dynamically Reconfigurable Intersection Test Hardware. In *ReCoSoc'08*.

Robbins, S. and Whitesides, S. (2003). On the reliability of triangle intersection in 3d. In *ICCSA (3)*, pages 923–930.

Shewchuk, J. R. (1997). Adaptive precision floating-point arithmetic and fast robust geometric predicates. *Discrete & Computational Geometry*, 18(3):305–368.

Weller, R., Klein, J., and Zachmann, G. (2006). A model for the expected running time of collision detection using aabb trees. In *Eurographics Symposium on Virtual Environments (EGVE)*, Lisbon, Portugal.

Woulfe, M., Dingliana, J., and Manzke, M. (2007). Hardware accelerated broad phase collision detection. In *SIGGRAPH 2007*, New York, USA. ACM SIGGRAPH.

Zachmann, G. (1998). Rapid Collision Detection by Dynamically Aligned DOP-Trees. *Proc. of IEEE, VRAIS'98 Atlanta.*